Advances in Science and Technology Research Journal

Advances in Science and Technology Research Journal 2023, 17(6), 1–15
https://doi.org/10.12913/22998624/172003
ISSN 2299-8624, License CC-BY 4.0

Received: 2023.07.26
Accepted: 2023.09.07
Published: 2023.11.21

Analysis of the Possibility of Using Neural Networks to Monitor the Technical Efficiency of Diesel Engines During Operation

Karol Tucki[1*], Olga Orynycz[2*], Antoni Świć[3], Andrzej Wasiak[4], Remigiusz Mruk[1], Arkadiusz Gola[3]

[1] Warsaw University of Life Sciences, Institute of Mechanical Engineering, Department of Production Engineering, Nowoursynowska Str. 164, 02-787 Warsaw, Poland

[2] Bialystok University of Technology, Faculty of Engineering Management, Department of Production Management, Wiejska Str. 45A, 15-351 Bialystok, Poland

[3] Department of Production Computerisation and Robotisation, Faculty of Mechanical Engineering, Lublin University of Technology, Nadbystrzycka Str. 36, 20-618 Lublin, Poland

[4] Advisors Panel Production Engineering, Alternative Energy Sources Bialystok, 15-351 Bialystok, Poland

* Corresponding author's e-mail: karol_tucki@sggw.edu.pl, o.orynycz@pb.edu.pl

ABSTRACT

The aim of the research was to analyse the possibility of using neural networks to determine the parameters of the chemical composition of exhaust gases as a function of engine performance parameters obtained from the on-board diagnostics system such as crankshaft speed and engine load index. The subject of the study was a Fiat Panda car equipped with a 1.3 Multijet diesel engine and powered by pure diesel. The tests used the MAHA MET 6.3 exhaust gas analyser and the on-board diagnostics system OBD II. The obtained values of NO_x,O_2,CO_2 and PM measured behind the DPF were analysed. For the purpose of building a neural network model, preliminary studies were carried out in non-urban traffic (high-speed route). On the basis of the data obtained, processes of learning neural network structures with approximate properties with backward propagation of errors were carried out. Subsequently, tests were performed on the operational parameters of the vehicle and the chemical composition of exhaust gases in urban traffic. Analysis of the obtained values of the average parameters obtained during the measurement and on the basis of the prepared neural models allows determining the relative differences at the level of not more than 10 percent.

Keywords: DPF, engine, vehicle; biofuel, fuel.

INTRODUCTION

Growing environmental awareness among drivers and increasingly restrictive legal regulations make it necessary to continue the research on reducing vehicle emissions into the atmosphere [1, 2].

Diesel particulate filter (DPF) is installed in the exhaust systems of diesel engines. Its task is to purify flue gases from particulate matter [3, 4]. Since 2005, with the introduction of the Euro 4 standard, their use in diesel vehicles has been mandatory. Since 2014, filters have also been installed in petrol cars equipped with direct fuel injection [5, 6]. The particulate filter is the part of the exhaust system behind the catalytic converter. It is housed in a stainless steel housing. A ceramic filter body, inside which there are parallel channels, is placed in its centre. They form a grid and each of them is closed on one side (inlet or outlet). Therefore, the exhaust gas must pass through the porous walls of the inlet ducts in order to reach the exhaust pipes [7, 8].

The purpose of the DPF filter is to trap the particulate matter produced by the car engine. Particulate matter is a mixture of organic fractions,

soot from fuel combustion and unburned hydrocarbons. Particulate matter is considered to be exhaust components which leave the exhaust system in a non-gaseous state. Soot particles are most often emitted, having a carbon core that absorbs other small particles, e. g. nitrates, metals or sulphates [9, 10]. Along with the installation of the particulate filter, other components such as a broadband lambda sensor, temperature sensors, pressure sensor must also be installed.

The operation of the DPF is monitored by several independent sensors. Their placement depends on the make of the car. The most important sensors in the exhaust aftertreatment system are pressure sensors. Two types of them can be distinguished. Some are responsible for measuring the pressure only in front of the filter. The latter check them before and after the DPF [11].

The device that is used in high spring motors is DPF, which is a dry filter. It is also possible to use a FAP filter (Filtre A Particules). This is the so-called wet particulate filter. Its structure and principle of operation is similar to DPF, but it also has a catalytic fluid tank, pump, injection, which allow reducing the firing temperature to about 400 degrees Celsius. Both types of devices have the same task, i.e. removing contaminants [12, 13]. From the point of view of the principles of operation, there are no differences [14,15].

The DPF filter and catalytic converter are designed to capture harmful substances from exhaust gases, but they work differently. The differences between the catalytic converter and the filter are visible in the structure of these elements, failure rate and operating principles. The catalyst has a cartridge with precious metals and undergoes chemical reactions with the exhaust gases to remove harmful substances from them. The particulate filter captures impurities and burns them off.

There are several ways of regenerating the particulate filter: passive regeneration (in which soot is neutralised automatically during a longer drive), active regeneration (it is triggered by a controller that increases the fuel dose and increases the engine speed), forced regeneration (the car plugs into a computer and drastically increases the exhaust gas temperature. This type of regeneration damages the engine, so it is done as a last resort). A cheap and effective way to regenerate DPF is the hydrodynamic method. Its advantages include, for example, that the parameters of the filters are restored to values almost the same as the factory ones. Washing effectively removes soot and ash [16, 17].

It is possible to remove the filter, but this is illegal. For driving a car with a DPF filter removed, one can be punished with a criminal fine and loss of a registration card. In Poland, this is punishable by a fine of PLN 5 thousand. If such a modification comes to light, e.g. at a diagnostic station, the car will not pass the registration check.

The manuscript presents the results of studies aimed at analysing the possibility of using neural networks to determine the parameters of the chemical composition of exhaust gases as a function of engine performance parameters obtained from the on-board diagnostics system, such as crankshaft speed and engine load index.

MATERIALS AND METHOD

The aim of the paper and the extent of research

Tests of operating parameters and chemical composition of exhaust gases were carried out on the 1.3 Multijet diesel engine. The exhaust gas was collected by means of a probe, which was inserted into the exhaust system and fed to the exhaust gas analyser mounted in the trunk of the vehicle.

Assumptions of research methodology:

- The extra-urban tests were carried out at different pre-set vehicle speeds (80 km/h, 90 km/h, 100 km/h, 110 km/h, 120 km/h) and at different engine load rates for the prevailing driving conditions;
- Urban traffic tests were carried out according to road conditions for high dynamics of vehicle speed and engine load. Each attempt lasted 300 seconds;
- The data on engine crankshaft speed, engine load index were obtained from the OBD II system, while exhaust gas composition was obtained from the exhaust gas analyser. This information was saved every 1 second;
- The engine temperature during the tests oscillated within the range of 90–95 °C.

Exhaust gas components were tested:

- CO_2 [%] – carbon dioxide;
- O_2 [%] – oxygen;
- NO_x [ppm] – oxides of nitrogen;
- PM [mg/m^3] – solid particles.

Test setup

Table 1 presents the basic technical characteristics of the Fiat 1.3 Multijet engine used in the tests. Apparatus used in the tests:

- Emission probe;
- Emission Software Program;
- Maha Met 6.3 exhaust gas analyser;
- OBD II (On Board Diagnostic).

The computer program that was included in the basic set of the exhaust gas analyser was connected to the analyser via wi-fi. The probe was connected to the analyser, while the OBD II was inserted into a special connector in the centre of the vehicle [20]. Table 2 shows the technical parameters of the Maha Met 6.3 exhaust gas analyser.

Maha Emission Software, which is the software included in the basic set of the MAHA Met 6.3 exhaust analyser, has the ability to measure vehicle exhaust emissions in vehicles with spark ignition and compression ignition engines. The software determines the measured values from the OBD device, which is connected to the Wifi network program. An important stage of the test is the leak test. At this level, the program checks that all connectors that are connected are tight and have no gaps or gaps. OBD II must be connected at the appropriate location on the vehicle. For the tests and used Fiat Panda, the space for the connector was on the left side of the steering wheel. If the device has been installed correctly, the light should turn blue. When everything is connected correctly, the program generates values such as NO, O_2, NO_x, PM, CO, CO_2 and HC. It also displays rotational speed, making it easier to measure and test parameters at different speeds.

Table 1. Basic technical data of the engine 1.3 Multijet II [18, 19]

Parameter	Description	Unit
Vehicle (MY, make, model)	Fiat Panda 1.3 Multijet II 16V 75	-
Equivalent test mass	1170	kg
Rated power (declared)	55	kW
Rated engine speed (declared)	4000	min^{-1}
Idling engine speed (declared)	800	min^{-1}
Max vehicle speed(declared)	168	km/h
Number of gears	5	-

Table 2. Basic technical data of the Maha Met 6.3 [21]

Power supply, input to Maha Met 6.3	
Supply voltage	10 - 30 V DC
Power consumption	60 W
AC adapter (included)	
Voltage	90 - 265 V DC
Load	60 W
Other information Maha Met 6.3	
Warm-up time	About 2 min.
Calibration gas connection	min. 0.5 bar to max. 1.0 bar; 0.5 to 1.5 l/min
Probe tube connector	Nominal flow rate: 5.5 l/min; minimum 4 l/min
Operating temperature	+5 to +45 °C
Storage temperature	−10 to +60 °C
Relative humidity	No condensation
Dimensions	406 × 220 × 160 mm
Weight	406 × 220 × 160 mm
Interfaces	LAN, optional WiFi

The studies used Scilab version 2023. 1.0 free and open source software for engineers and scientists together with the Neural Network Module version 3.0.

For the construction of the neural model, neural network structures "Multilayer Feedforware Backpropagation Network" with approximating properties were used.

A characteristic feature of these networks, the general scheme of which is shown in Figure 1, is the presence of at least one hidden layer of neurons, which mediates the transmission of signals between the input nodes and the output layer. The input signals are fed to the first hidden layer of neurons, and these in turn are the source signals for the next layer. There are full connections between the layers.

In the structure of the neural network, the nonlinear activating functions $f_1(x)$ and $f_2(x)$ are applied in the hidden layers and the linear activating function $f_3(x)$ in the form of:

$$f_1(x) = \frac{2}{1 + \exp(-2\sum_{i=1}^{n} w_i x_i + b_i)} \quad (1)$$

$$f_2(x) = \frac{2}{1 + \exp(-2\sum_{i=1}^{n} u_i x_i + b_i)} \quad (2)$$

$$f_3(x) = \sum_{i=1}^{n} v_i x_i + b_i \quad (3)$$

where: b_i – polarity values of neurons in individual layers;
x_i – input signals for the neuron;
w_i, u_i, v_i – weight values of neurons in individual layers.

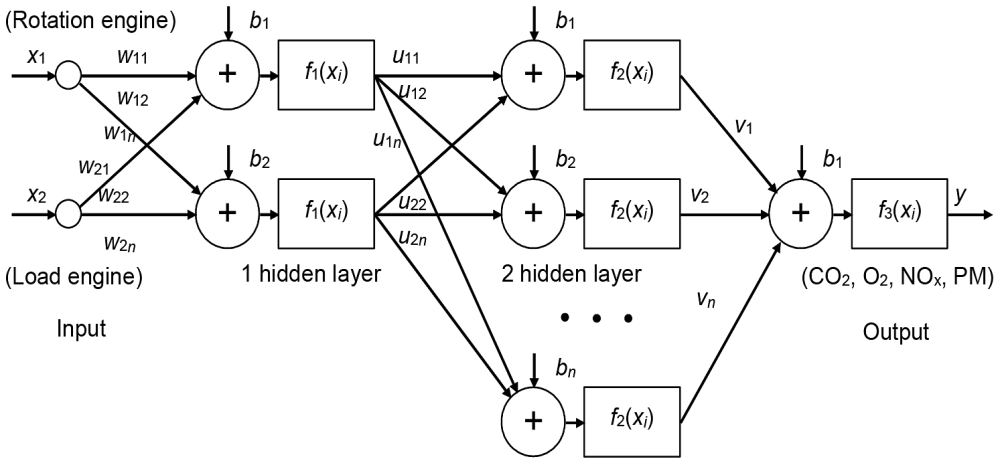

Fig. 1. Schematic of the one-way, multilayer neural network with approximate features, which was used to build neural models: x_i – input signals for the neuron; w_i, u_i, v_i – weight values of neurons in individual layers; b_i – polarity values of neurons in individual layers; y_i – given learning values

During the network learning process, the Levenberg–Marquardt algorithm was used, which is based on the optimisation process by finding the minimum value of the target function defined as the mean value of the sum of squares of the differences between the current values of the network output signals and the values set in the form of equation 4. An analysis of the source code of Neural Network Module version 3.0 revealed that the learning functions contained therein only calculate the Mean square error rate during the learning process. Only this indicator can be obtained directly after the completion of the learning process for further study stages. If other indicators (RMSE, MAE) are used, it would be necessary to modify the source code and recompile the library by the user. Additional modifications to the Neural Network Module were not performed within the scope of the study.

$$\Delta\bar{e}^2 = \frac{1}{m}\sum_{i=1}^{m}(d_i - y_i)^2 \tag{4}$$

where: y_i – given learning values;
d_i – values of network responses in the learning process.

Before the processes of learning and testing neural network structures, all input data were subjected to a normalisation process, so that the calculated values met the criteria of the <0-1> range. The presented results of neural network learning processes in the form of the Mean square error indicator refer to normalised data.

The learning and testing of neural networks used data from real-world extra-urban driving tests, including 5 cases of vehicle behaviour for different vehicle speeds (80 km/h, 90 km/h, 100 km/h, 110 km/h, 120 km/h). Two cases of independent tests were used to compare the obtained neural models and real city traffic tests for the content of selected exhaust gas components.

In the process of learning the described neural network to obtain a model of carbon dioxide content in exhaust gases, training data from mobile tests were used containing a selected set of 400 measuring points. Subsequently, in order to obtain the most accurate neural model for real data, studies were carried out with the size of 2 hidden layer networks ranging from 1 to 6 neurons. The learning process for each network size was repeated 100 times and a maximum iteration value of 10000 was set. Then, on the basis of the obtained Mean square error (correlation coefficients R^2) for individual learned neural networks to the test data (400 measurement points), the neural networks with the best fit but not yet having the characteristics of overlearning (data interpolation) were selected. The same procedure was carried out for the other parameters analysed. In order to automate the learning processes of networks of different sizes, verify learned networks, write networks to disk, generate results in the form of graphs and tests, the necessary programs have been developed in the Scilab environment. In the analysed case, 400 points were tested/validated.

Table 3 shows the sizes of neural networks and their results of matching the Mean square error and correlation coefficients R^2 to the data that

Table 3. Results of the selection process of optimal neural network sizes

Neural network model	Neural network size (layer 1/layer 2)	Mean square error	Correlation coefficient R^2
CO_2 [%]	2 / 4	1.066e-5	0.971
O_2 [%]	2 / 4	1.064e-5	0.968
NO_x [ppm]	2 / 2	2.549e-5	0.955
PM [mg/m^3]	2 / 3	1.401e-4	0.947

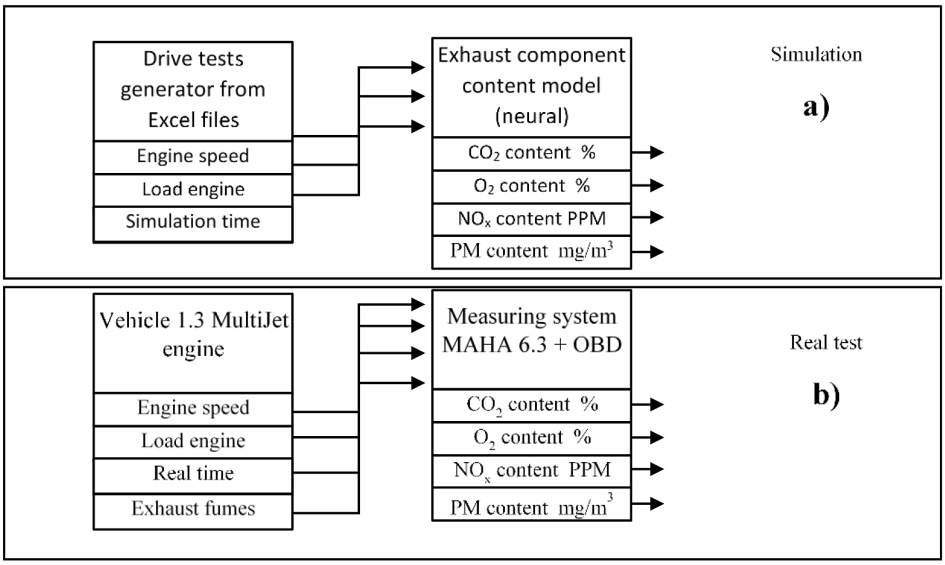

Fig. 2. General scheme of the test method: a – computer simulation; b – laboratory measurement

were used to try to simulate the content of analysed components for urban traffic tests. Figure 2 shows the diagrams of how the tests are carried out: simulation system for the content of analysed components in exhaust gas using neural network models and diagram of the measuring system allowing the collection of the vehicle performance parameters and the contents of the exhaust components during the vehicle operation.

RESEARCH RESULTS

The tests were carried out on a Fiat Panda 1.3 Multijet equipped with a diesel engine. The results of the tests are presented in graphs and tables. Tests were carried out for different engine speeds and emissions were tested behind the particulate filter.

Engine operating parameters

Figure 3 shows the waveforms of the instantaneous engine speed values obtained from the OBD system when the vehicle is driving on an urban road. Figure 4 shows the waveforms of the instantaneous load engine values obtained from the OBD system when the vehicle is driving on a city road.

CO_2 content of exhaust gases

In the work undertaken, using a neural model, on the basis of instantaneous values of the engine load index and engine speed, instantaneous values of the share of CO_2 in exhaust gases are obtained according to the relationship:

$$CO_2 = \mathrm{f_{Net}}\begin{pmatrix} Rotation_{\mathrm{engine}}, \\ \mathrm{Load_{engine}} \end{pmatrix} [\%\mathrm{V/V}] \quad (5)$$

In the same way, models based on neural network structures for the content of O_2, NO_x and PM in exhaust gases were built. Figure 5 shows the model of the carbon dioxide content in the exhaust gas as a function of engine speed and load obtained using neural networks with approximating properties. In order to verify the functioning of the neural model of the carbon dioxide content in the exhaust gas (Figures 6 and 7) as a function of rotational speed and engine load index, the vehicle was driven twice (two runs) in urban traffic (designated in the graphs as Test 1 and Test 2).

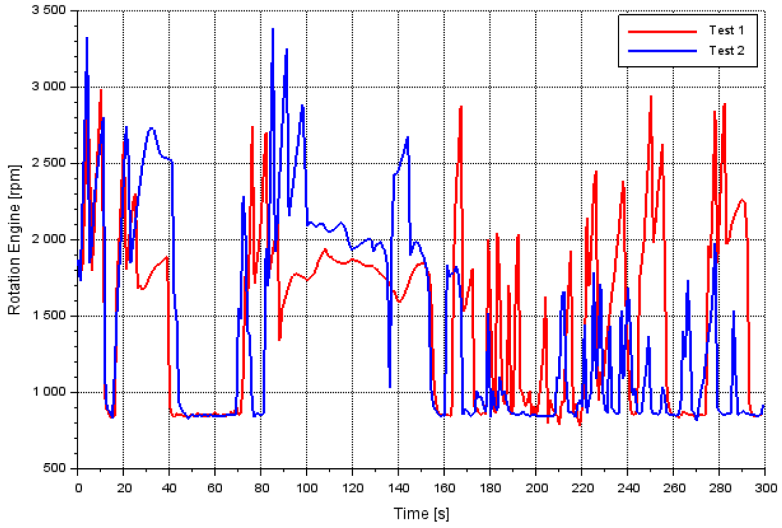

Fig. 3. Waveforms of the instantaneous engine speed values obtained from the OBD system: red colour – test 1, blue colour – test 2

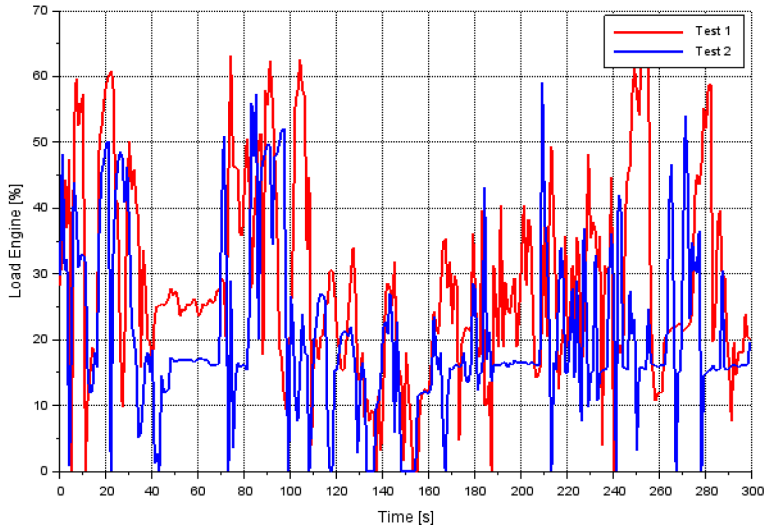

Fig. 4. Waveforms of the instantaneous load engine values obtained from the OBD system: red– test 1, blue– test 2

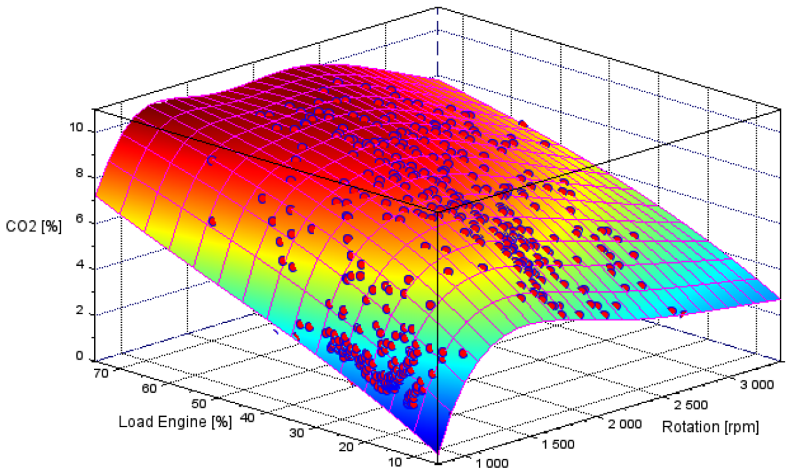

Fig. 5. Surface showing the developed model using the neural network of changes in CO_2 content in the exhaust gas as a function of engine speed and load engine (red points engine performance parameters obtained during tests 1, 2)

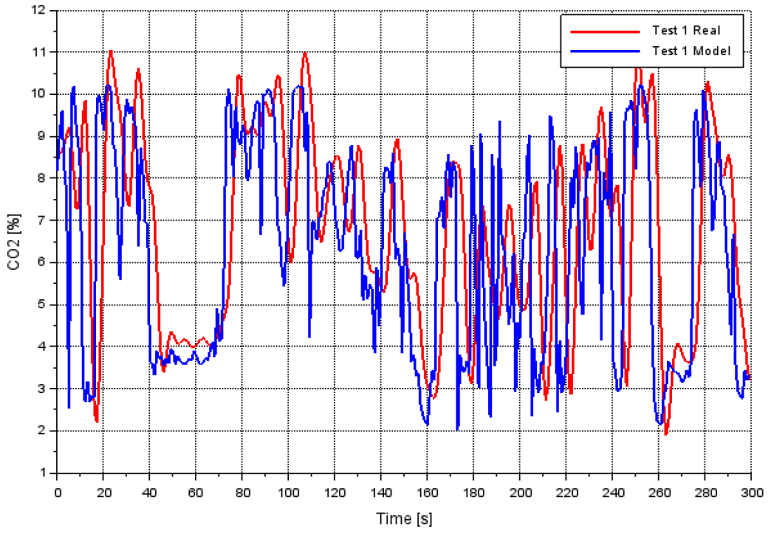

Fig 6. Test 1 – waveforms of instantaneous carbon dioxide CO_2 content in exhaust gases: red – readings from exhaust gas analyser, blue –neuronal model

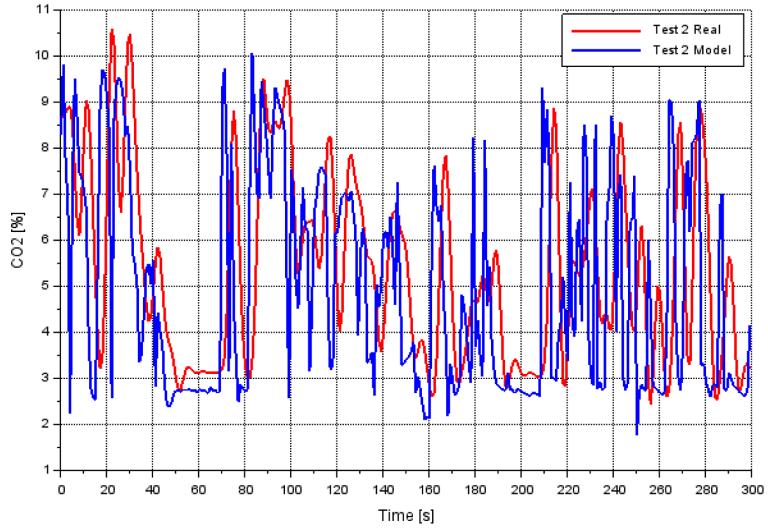

Fig. 7. Test 2 – waveforms of the instantaneous CO_2 content in the exhaust gas: red – values read from the exhaust gas analyser, blue – neuronal model

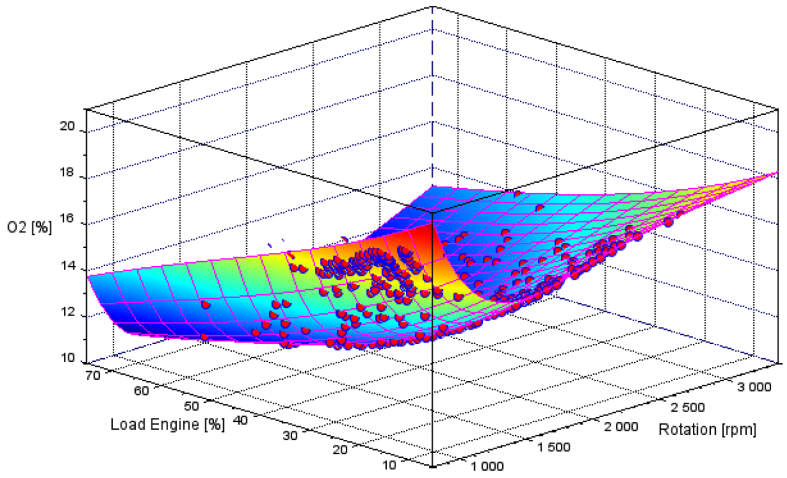

Fig. 8. Surface showing the model developed using the neural network of changes in O_2 in the exhaust gas as a function of rotational speed and Load Engine (red points engine performance parameters obtained during tests 1, 2)

O_2 content in exhaust gas

Figure 8 shows the model of the oxygen content of the exhaust gas as a function of engine speed and load obtained using neural networks with approximating properties. The results of the comparison of the values obtained from the measurements and from the neural model are shown in Figures 9 and 10.

NO_x content in exhaust gas

Figure 11 shows the model of nitrogen oxides in the exhaust gas as a function of engine speed and load using neural networks with approximating properties. The results of the comparison of the values obtained from the measurements and from the neural model are shown in Figures 12 and 13.

PM content in exhaust gas

Figure 14 shows a model of the particulate content of the exhaust gas as a function of engine speed and load using neural networks with approximating properties. The results of the comparison of the values obtained from the measurements and from the neural model are shown in Figures 15 and 16.

Summary of test results

Table 4 summarises the mean values of the analysed parameters obtained during the

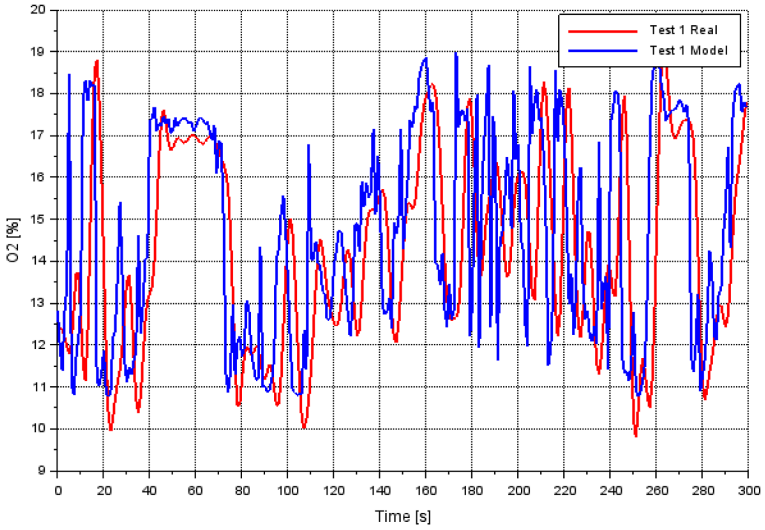

Fig. 9. Test 1 – waveforms of instantaneous O_2 content in exhaust gas: red – values read from exhaust gas analyser, blue – neural model

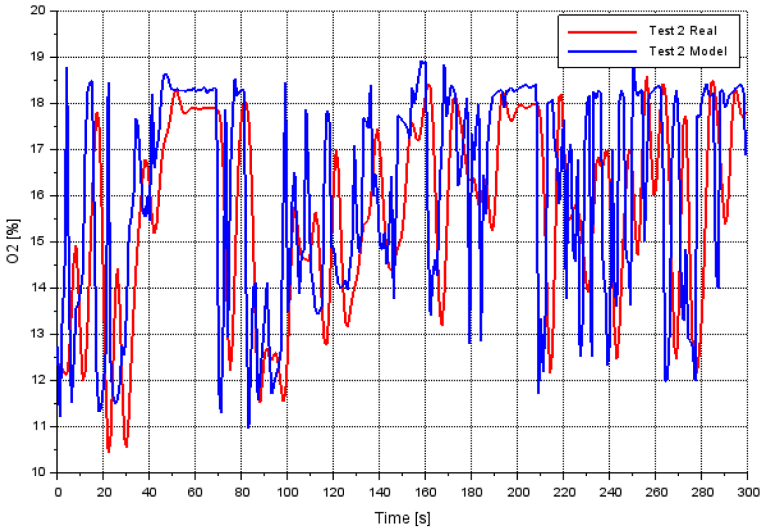

Fig. 10. Test 2 – waveforms of instantaneous O_2 content in exhaust gas: red – values read from exhaust gas analyser, blue – neural model

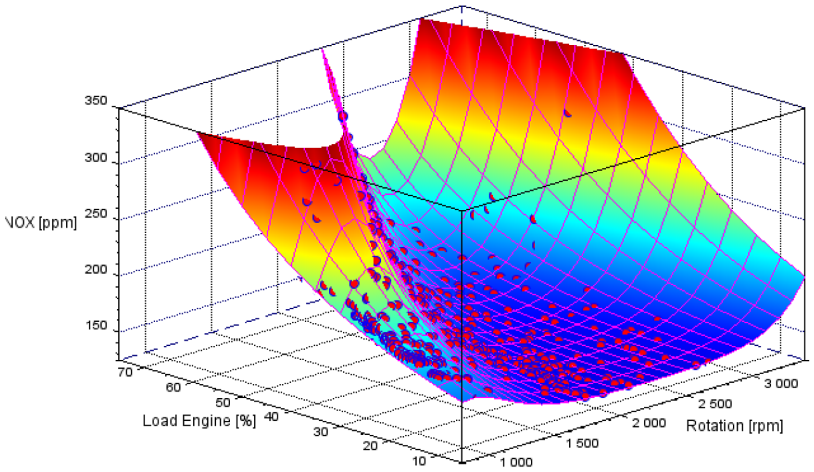

Fig. 11. Surface showing the model developed using the neural network of changes in NO_x in the exhaust gas as a function of speed and load engine (red points engine performance parameters obtained during tests 1, 2)

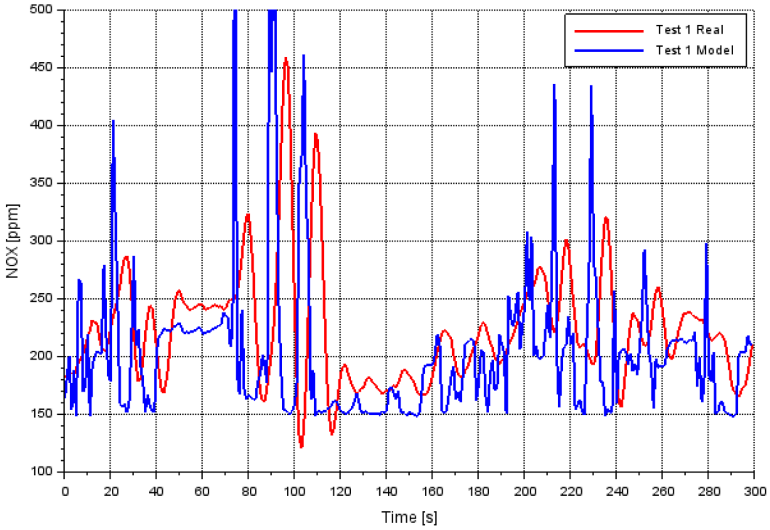

Fig. 12. Test 1 – waveforms of instantaneous nitrogen oxides NO_x in exhaust gas: red – values read from exhaust gas analyser, blue – neuronal model

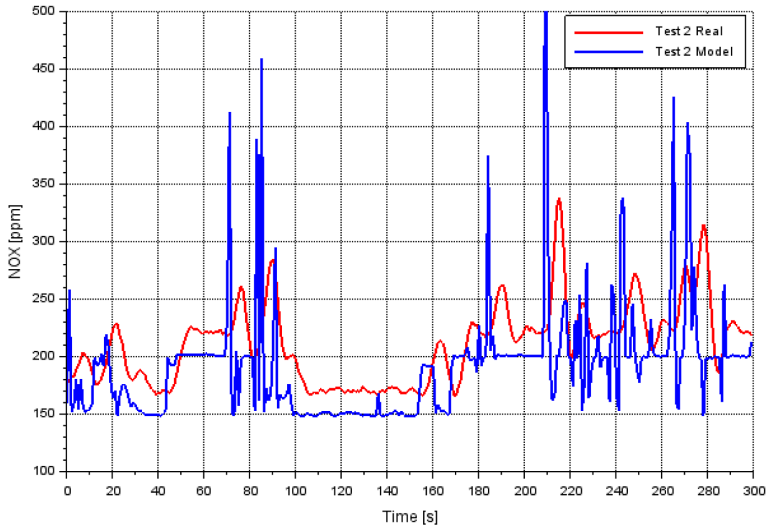

Fig. 13. Test 2 – waveforms of instantaneous nitrogen oxides NO_x in exhaust gas: red – values read from exhaust gas analyser, blue – neuronal model

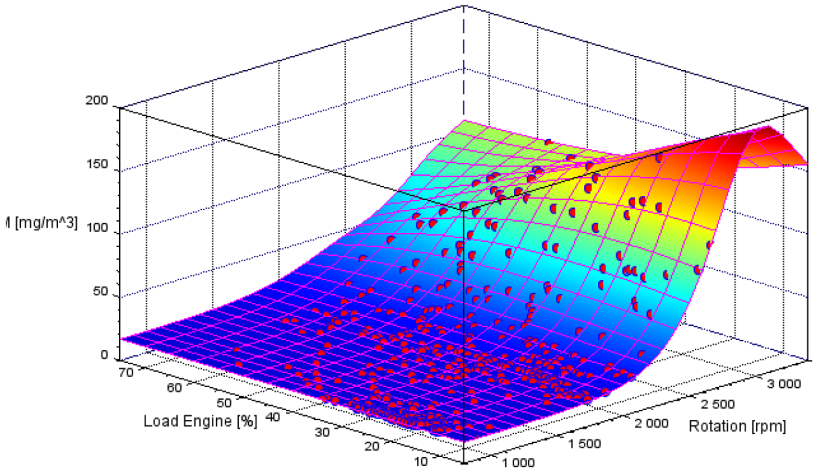

Fig. 14. Surface showing the model developed using the neural network of changes in particulate content in the exhaust gas as a function of rotational speed and load engine (red points engine performance parameters obtained during tests 1, 2)

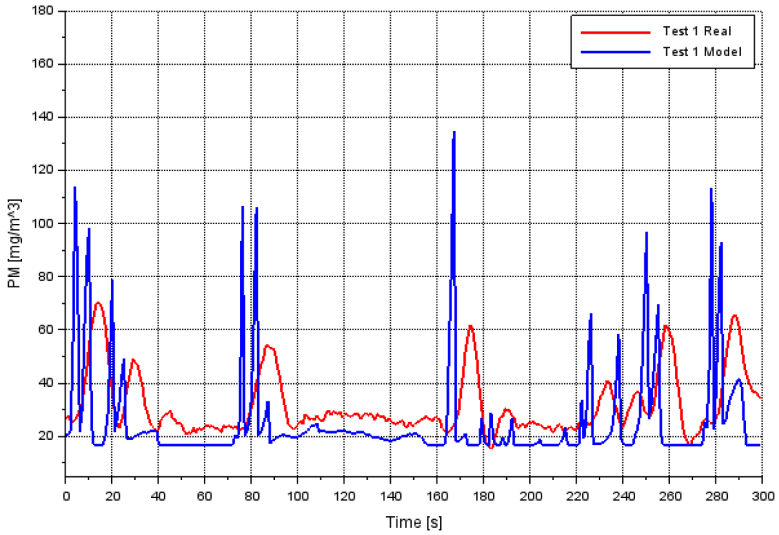

Fig. 15. Test 1 – waveforms of instantaneous particulate content in exhaust gas [mg/m^3]: red – values read from exhaust gas analyser, blue – neuronal model

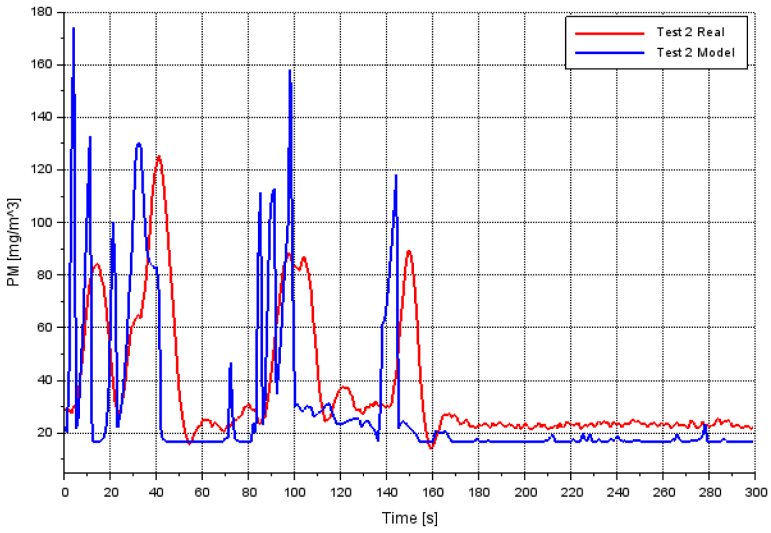

Fig. 16. Test 2 – waveforms of instantaneous particulate content in exhaust gas [mg/m^3]: red – values read from exhaust gas analyser, blue – neuronal model

Table 4. Summary of average values

Test number	Type of test	CO_2 [%]	O_2 [%]	NO_X [ppm]	PM [mg/m^3]
Test 1	Obtained from measurements	6.76	14.2	222	31.4
Test 1	Obtained from model	6.30	14.7	202	25.4
Test 2	Obtained from measurements	5.38	15.6	210	36.6
Test 2	Obtained from model	4.93	16.1	191	30.4

measurement and obtained on the basis of the prepared neural models. The mean values shown in Table 3 show that for CO_2, O_2, NO_x, the relative error of the values obtained using neural networks in relation to the measurements did not exceed 10 percent. For PM, the error was twice as large.

DISCUSSION

The studies presented in the manuscript were carried out using standard diesel fuel. The studies used a network-based neural model with backward propagation of errors and the results of mobile tests carried out using the Maha 6.3 exhaust gas analyser in urban traffic. As a result of the analysis of the obtained parameters and their verification, the relative errors of the percentage content of the analysed exhaust gas components were found at a level not exceeding several percent. This approach allows pre-tests to be carried out using fuels with different bio-additive content [22, 23]. It will also be possible to use neural models to determine the chemical composition of exhaust gases based on measurement data. Neural models are used to reproduce the tests that take into account technical parameters of vehicles, compositions of fuel mixtures.

From the point of view of CO_2 emissions, it is important to consider the use of biofuels. Nevertheless, the modern diesel engine has been designed and refined for the combustion of mineral diesel, which has different physicochemical properties. The use of crude rapeseed oil requires special adaptation of injection systems and combustion chambers [24, 25]. Under Polish climatic conditions, the main source of plant esters was rapeseed oil. Rapeseed oil methyl esters are the fuel with physical properties closest to diesel.

Frying oils are known as UCO (used cooking oil) [26]. They are a mixture of animal and vegetable fats formed mainly as a result of the so-called deep-fat frying [27, 28]. In Europe, rapeseed, palm, soy and sunflower oils are used for frying, in addition to all kinds of butter, margarine and lard. After the initial thermal treatment and filtration process, this oil is mainly used as a heating fuel, and more recently as a raw material for the production of methyl esters [29, 30]. Frying oils as well as animal oils are currently the largest alternative to other raw materials for the production of methyl esters such as rapeseed, palm or soybean oils [31-33].

Higher Fatty Acid Methyl Esters (FAME) are also used to power compression ignition engines and can be blended in appropriate proportions with petroleum diesel [34, 35]. Such fuel is used as a few percent blends with conventional fuel or as a stand-alone B100 fuel [36]. FAME, like conventional fuels, has a tendency to solidify (crystallise) at low temperatures [37]. This process causes loss of fluidity and solidification of the fuel [38, 39].

Due to its promising environmental properties, the use of the butyl alcohol derived from biomass (biobutanol) as a substitute for conventional diesel is subject to increasing verification [40, 41]. The raw materials are energy crops such as sugar beets, sugar cane, corn grains, wheat and cassava, as well as agricultural and forestry by-products such as straw, corn stalks and wood waste [42]. Biobutanol is obtained by fermentation under anaerobic conditions similar to ethanol, but with the use of other microorganisms in the process [43-45]. In ethanol production, these are primarily yeasts – single-celled fungi that produce enzymes to break down carbohydrates, and in the case of butanol – bacterial strains [46, 47]. Butanol is more energy efficient than ethanol, because it contains more carbon.

Commonly used biocomponents, such as bioethanol and fatty acid methyl esters (FAME), are called first generation biofuels [48]. In line with EU policy in recent years, emphasis has been placed on the development of new technologies for converting inedible raw materials, waste materials into second-generation biofuels (e.g. from lignocellulosic waste) and third-generation biofuels from dedicated bio-processes [49, 50].

Application of dedicated neural models in vehicle embedded systems may be the basis for developing systems for rapid diagnostics of selected vehicle components. Computer tools are also an excellent basis for conducting preliminary tests on the effect of the fuel mixture composition on the engine and exhaust system of a vehicle.

The authors of the manuscript have been using neural networks and genetic algorithms in their research for many years. They used the support of artificial intelligence methods, for example, to model numerical flows in turbine stages [51, 52], to model vehicle driving tests [53, 54]. The authors of the manuscript in published scientific papers have analysed a wide range of different approval procedures carried out on vehicles with compression ignition and spark ignition engines, taking into account different fuel mixtures and equipment with assistance systems, e.g. start-stop system [55, 56]. For the purpose of achieving the set research goals, proprietary computational tools created in OpenModelica, Scilab, Matlab packages using artificial intelligence methods were used. Previous research results have shown that neural networks can support the modelling of exhaust emissions from motor vehicles. Given the dynamics of developments in the development of new fuel mixes, retrofitting of motor vehicles and changes in legislation on exhaust emission limits, further research into new computer tools using neural networks for exhaust emission modelling is urgently needed.

For many years, attempts have been made in science to use artificial neural networks wherever the complex nature of the problems prevents or significantly prolongs the analysis of the problem presented in a classical, mathematical way. Moreover, the literature review notes gaps in the issues related to strength analysis, thermodynamics, heat exchange and technical operation.

In the process of operation of modern internal combustion engines, a number of different methods and techniques are used to detect early stages of failures and increase their efficiency and reliability, e.g. modal analysis of mechanical objects, simultaneous analysis of time and frequency properties of signals using a wave transform, satellite monitoring systems, OBD systems (On-Board Diagnostics).

The effectiveness of OBD systems capable of detecting mechanical engine failures masked by electronic controls of modern motor vehicles can be enhanced by the development of systems using artificial neural networks.

CONCLUSIONS

On the basis of the conducted research, it can be concluded that:

1. The neural network models used to determine the content of selected components of exhaust gases due to the accuracy obtained in relation to the measured values allow using them in applications to determine the technical condition of the vehicle engine.
2. The use of mobile exhaust gas analysers allows carrying out measurements in actual urban and non-urban traffic conditions. It is the only way in the absence of access to chassis dynamometers.
3. The obtained relative errors of the neural models in relation to the real values indicate the need for more detailed studies and to take into account more operational parameters of the engine and the vehicle structure (temperature of the air sucked into the engine, charge pressure, etc.).

Acknowledgments

The research was carried out under financial support obtained from the research subsidy of the Faculty of Engineering Management (WIZ) of Bialystok University of Technology, grant No. WZ/WIZ-INZ/4/2022 (Olga Orynycz). This research was also funded by the Institute of Mechanical Engineering, Warsaw University of Life Sciences.

REFERENCES

1. Nieuwenhuijsen MJ. Urban and transport planning pathways to carbon neutral, liveable and healthy cities; A review of the current evidence. Environment International 2020;140:105661. https://doi.org/10.1016/j.envint.2020.105661
2. Puricelli S, Cardellini G, Casadei S, Faedo D, Van den Oever AEM, Grosso M. A review on biofuels for light-duty vehicles in Europe. Renewable and Sustainable Energy Reviews 2020;137:110398. https://doi.org/10.1016/j.rser.2020.110398
3. Phyo MZM, Wai P, Thin MH, Oh BS, Phairote W, Srilomsak M, Charoenphonphanich C, Masomtob M, Srimanosaowapak S, Kosaka H, Karin P. Experimental investigation of metallic partial-flow particulate filter on a diesel engine's combustion pressure and particle emission. Case Studies in Thermal Engineering 2023; 49:103188. https://doi.org/10.1016/j.csite.2023.103188
4. Meng Z, Wang W, Zeng B, Bao Z, Hu Y, Ou J, Liu J. An experimental investigation of particulate

emission characteristics of catalytic diesel particulate filters during passive regeneration. Chemical Engineering Journal 2023; 468:143549. https://doi.org/10.1016/j.cej.2023.143549

5. Zerboni A, Rossi T, Bengalli R, Catelani T, Rizzi C, Priola M, Casadei S, Mantecca P. Diesel exhaust particulate emissions and in vitro toxicity from Euro 3 and Euro 6 vehicles. Environmental Pollution 2022; 297:118767. https://doi.org/10.1016/j.envpol.2021.118767
6. Huang Y, Ng ECY, Surawski NC, Zhou JL, Wang X, Gao J, Lin W, Brown RJ. Effect of diesel particulate filter regeneration on fuel consumption and emissions performance under real-driving conditions. Fuel 2022; 320:123937. https://doi.org/10.1016/j.fuel.2022.123937
7. Zhu X, Liu S, Wang Z, Li R, Zhao Z. Study of the influence of methanol/F-T diesel combustion particle materiality parameters on the deposition process in diesel particulate filter trap units. Journal of the Energy Institute 2023; 107:101184. https://doi.org/10.1016/j.joei.2023.101184
8. Kumar MV, Babu AV, Reddy CR, Pandian A, Bajaj M, Zawbaa HM, Kamel S. Investigation of the combustion of exhaust gas recirculation in diesel engines with a particulate filter and selective catalytic reactor technologies for environmental gas reduction. Case Studies in Thermal Engineering 2022;40:102557. https://doi.org/10.1016/j.csite.2022.102557
9. Liu D, Li X, Xie L, Chang J, Kang Y, Zhang Z. Experimental studies on the particulate matter emission characteristics of a lateral swirl combustion system for direct injection diesel engines. Environmental Pollution 2023;330:121756. https://doi.org/10.1016/j.envpol.2023.121756
10. Lou D, Chen Y, Zhang Y, Jue K, Tan P, Hu Z, Fang L. Analysis of temperature and pressure characteristics in catalyzed diesel particulate filter operation for heavy-duty diesel engine. Fuel 2022;328:125248. https://doi.org/10.1016/j.fuel.2022.125248
11. Ashraful AM, Masjuki HH, Kalam MA, Rashedul HK, Sajjad H, Abedin MJ. Influence of anti-corrosion additive on the performance, emission and engine component wear characteristics of an IDI diesel engine fueled with palm biodiesel. Energy Conversion and Management 2014;87:48-57. https://doi.org/10.1016/j.enconman.2014.06.093
12. Wójcik M. Recycling technologies of used Diesel Particulate Filter (DPF) from buses. Autobusy 2017;10:29-33.
13. Durczak T, Sander P, Górski K. Analysis of exhaust after-treatment systems and methods of their regeneration. Autobusy 2017;12:829-832.
14. Fuć P, Siedlecki S, Szymlet N, Sokolnicka B, Rymaniak Ł, Dobrzyński M. Exhaust emissions from a Euro 6c compliant pc vehicle in real operating conditions. Journal of KONBiN 2019;49:421-431. 10.2478/jok-2019-0094
15. Bielaczyc P, Szczotka A, Woodburn J. An overview of particulate matter emissions from modern light duty vehicles. Combustion Engines. 2013;153(2):101-108. doi:10.19206/CE-117007
16. Kurien C, Srivastava AK, Naudin J. Modelling of regeneration and filtration mechanism in diesel particulate filter for development of composite regeneration emission control system. Archive of Mechanical Engineering 2018; LXV: 277-290. DOI 10.24425/123025
17. Zuo Q, Gong J, Zhang DM, Chen T, Jia G. Performance evaluation on field synergy and composite regeneration by coupling cerium-based additive and microwave for a diesel particulate filter. Journal of Central South University 2014;21(12):4599–4606. DOI: 10.1007/s11771-014-2466-6
18. Ambrozik A, Ambrozik T, Kurczyński D. Load characteristics of turbocharged 1.3 Multijet engine. Advances in Science and Technology 2012; 15: 7–20.
19. Ambrozik A, Kurczyński D, Łagowski P, Warianek M. The toxicity of combustion gas from the Fiat 1.3 Multijet engine operating following the load characteristics and fed with rape oil esters. Proceedings of The Institute of Vehicles 2016; 1: 23–36
20. OBD2. Available online: https://www.csselectronics.com/pages/obd2-pid-table-on-board-diagnostics-j1979 (accessed on 19 June 2023)
21. MAHA. Emission measurement technology. Available online: https://www.maha.de/restriction/check-asset/support_documents/dokumente/Brosch%C3%BCren/MAHA/05_Abgasmesstechnik/MET/TD_MAHA_MET_6.3_VP135213_en.pdf (accessed on 19 June 2023)
22. Gao J, Chen H, Li Y, Chen J, Zhang Y, Dave K, Huang Y. Fuel consumption and exhaust emissions of diesel vehicles in worldwide harmonized light vehicles test cycles and their sensitivities to eco-driving factors. Energy Conversion and Management 2019; 196: 605-613. https://doi.org/10.1016/j.enconman.2019.06.038
23. Krause J, Thiel C, Tsokolis D, Samaras Z, Rota C, Ward A, Prenninger P, Coosemans T, Neugebauer S, Verhoeve, W. EU road vehicle energy consumption and CO2 emissions by 2050 – Expert-based scenarios. Energy Policy 2020; 138: 111224. https://doi.org/10.1016/j.enpol.2019.111224
24. Tucki K, Bączyk A, Klimkiewicz M, Mączyńska J, Sikora M. Crude rapeseed oil as a fuel for vehicle propulsion. IOP Conference Series. Earth and Environmental Science 2019; 214: 1-10. doi:10.1088/1755-1315/214/1/012103
25. Kim K., Lee J., Kim J. Can liquefied petroleum gas vehicles join the fleet of alternative fuel vehicles? Implications of transportation policy based on

market forecast and environmental impact. Energy Policy 2021; 154: 112311. https://doi.org/10.1016/j.enpol.2021.112311

26. Foteinis S, Chatzisymeon E, Litinas A, Tsoutsos T. Used-cooking-oil biodiesel: Life cycle assessment and comparison with first- and third-generation biofuel. Renewable Energy 2020; 153:588-600. https://doi.org/10.1016/j.renene.2020.02.022.
27. Yahya NY, Ngadi N, Wong S, Hassan O. Transesterification of used cooking oil (UCO) catalyzed by mesoporous calcium titanate: Kinetic and thermodynamic studies. Energy Conversion and Management 2018;164:210-218. https://doi.org/10.1016/j.enconman.2018.03.011.
28. Muelas A, Remacha P, Ballester J. Droplet combustion and sooting characteristics of UCO biodiesel, heating oil and their mixtures under realistic conditions. Combustion and Flame 2019;203:190-203. https://doi.org/10.1016/j.combustflame.2019.02.014
29. Orjuela A, Clark J. Green chemicals from used cooking oils: Trends, challenges, and opportunities. Current Opinion in Green and Sustainable Chemistry 2020;26:100369. https://doi.org/10.1016/j.cogsc.2020.100369
30. Moazeni F, Chen MC, Zhang G. Enzymatic transesterification for biodiesel production from used cooking oil, a review. Journal of Cleaner Production 2019;216:117-128. https://doi.org/10.1016/j.jclepro.2019.01.181
31. Matbouei M, Weston DP, Liang X, Hainsworth SV. An investigation of the effect of temperature on the oxidation processes of metallic diesel engine fuel system materials and B100 biodiesel from used cooking oil in exposure testing. Fuel 2021;285:119063. https://doi.org/10.1016/j.fuel.2020.119063
32. Ghosh N, Halder G. Current progress and perspective of heterogeneous nanocatalytic transesterification towards biodiesel production from edible and inedible feedstock: A review. Energy Conversion and Management 2022;270:116292. https://doi.org/10.1016/j.enconman.2022.116292
33. Roslan NA, Abdullah N, Abidin SZ. The synthesis of sulphonated hypercrosslinked exchange resin for free fatty acid esterification. Comptes Rendus Chimie 2019;22:761-770. https://doi.org/10.1016/j.crci.2019.08.004
34. Bemani A, Xiong Q, Baghban A, Habibzadeh S, Mohammadi AH, Doranehgard MH. Modeling of cetane number of biodiesel from fatty acid methyl ester (FAME) information using GA-, PSO-, and HGAPSO- LSSVM models. Renewable Energy 2020;150:924-934. https://doi.org/10.1016/j.renene.2019.12.086
35. Gwardiak H, Rozycki K, Ruszkarska M, Tylus J, Walisiewicz-Niedbalska W. Evaluation of fatty acid methyl esters (FAME) obtained from various feedstock. Rośliny Oleiste Oilseed Crop 2011;32: 137–147.
36. Neto JAR, Alves SN, Lima L.Fatty acid methyl esters (FAMEs) obtained from edible vegetable oils: Larvicidal activity and melanization process in Aedes aegypti larvae. Biocatalysis and Agricultural Biotechnology 2023;50:102689. https://doi.org/10.1016/j.bcab.2023.102689
37. Niculescu R, Năstase M, Clenci A. On the determination of the distillation curve of fatty acid methyl esters by gas chromatography. Fuel 2022;314:123143. https://doi.org/10.1016/j.fuel.2022.123143
38. Liu W, Lu G, Yang G, Bi Y. Improving oxidative stability of biodiesel by cis-trans isomerization of carbon-carbon double bonds in unsaturated fatty acid methyl esters. Fuel 2019;242:133-139. https://doi.org/10.1016/j.fuel.2018.12.132
39. Ameen NHA, Durak E. Study of the tribological properties the mixture of soybean oil and used (waste) frying oil fatty acid methyl ester under boundary lubrication conditions. Renewable Energy 2020;145:1730-1747. https://doi.org/10.1016/j.renene.2019.06.117
40. Bharathiraja B, Jayamuthunagai J, Sudharsanaa T, Bharghavi A, Praveenkumar R, Chakravarthy M, Yuvaraj D. Biobutanol – An impending biofuel for future: A review on upstream and downstream processing tecniques. Renewable and Sustainable Energy Reviews 2017;68:788-807. https://doi.org/10.1016/j.rser.2016.10.017
41. Tsai TY, Lo YC, Dong CD, Nagarajan D, Chang JS, Lee DJ. Biobutanol production from lignocellulosic biomass using immobilized Clostridium acetobutylicum. Applied Energy 2020;277:115531. https://doi.org/10.1016/j.apenergy.2020.115531
42. Nandhini R, Rameshwar SS, Sivaprakash B, Rajamohan N, Monisha RS. Carbon neutrality in biobutanol production through microbial fermentation technique from lignocellulosic materials – A biorefinery approach. Journal of Cleaner Production 2023;413:137470. https://doi.org/10.1016/j.jclepro.2023.137470
43. Xue C, Zhao J, Chen L, Yang ST, Bai F. Recent advances and state-of-the-art strategies in strain and process engineering for biobutanol production by Clostridium acetobutylicum. Biotechnology Advances 2017;35:310-322. https://doi.org/10.1016/j.biotechadv.2017.01.007
44. Huzir NM, Aziz MMA, Ismail SB, Abdullah B, Mahmood NAN, Umor NA, Muhammad SAFS. Agro-industrial waste to biobutanol production: Eco-friendly biofuels for next generation. Renewable and Sustainable Energy Reviews 2018;94:476-485. https://doi.org/10.1016/j.rser.2018.06.036
45. Cabezas R, Duran S, Zurob E, Plaza A, Merlet G, Araya-Lopez C, Romero J, Quijada-Maldonado E.

Development of silicone-coated hydrophobic deep eutectic solvent-based membranes for pervaporation of biobutanol. Journal of Membrane Science 2021;637:119617. https://doi.org/10.1016/j.memsci.2021.119617

46. Barbosa TP, Eckert JJ, Roso VR, Pujatti FJP, Silva LAR, Gutiérrez JCH. Fuel saving and lower pollutants emissions using an ethanol-fueled engine in a hydraulic hybrid passengers vehicle. Energy 2021;235:121361. https://doi.org/10.1016/j.energy.2021.121361
47. Zhang M, Ge Y, Wang X, Xu H, Tan J, Hao L. Effects of ethanol and aromatic compositions on regulated and unregulated emissions of E10-fuelled China-6 compliant gasoline direct injection vehicles. Renewable Energy 2021;176:322-333. https://doi.org/10.1016/j.renene.2021.03.029
48. Makkawi Y, Khan M, Pour FH, Moussa O, Mohamed B, Alnoman H, Elsayed Y. A comparative analysis of second-generation biofuels and its potentials for large-scale production in arid and semi-arid regions. Fuel 2023;343:127893. https://doi.org/10.1016/j.fuel.2023.127893
49. Abbasi M, Pishvaee MS, Mohseni S. Third-generation biofuel supply chain: A comprehensive review and future research directions. Journal of Cleaner Production 2021;323:129100. https://doi.org/10.1016/j.jclepro.2021.129100
50. Yang Y, Tian Z, Lan Y, Wang S, Chen H. An overview of biofuel power generation on policies and finance environment, applied biofuels, device and performance. Journal of Traffic and Transportation Engineering (English Edition) 2021;8:534-553. https://doi.org/10.1016/j.jtte.2021.07.002
51. Kosowski K, Tucki K, Kosowski A. Turbine stage design aided by artificial intelligence methods. Expert Systems with Applications 2009;36: 11536-11542. https://doi.org/10.1016/j.eswa.2009.03.053
52. Kosowski K, Tucki K, Kosowski A. Application of Artificial Neural Networks in Investigations of Steam Turbine Cascades. Journal of Turbomachinery-Transactions of the ASME 2010;132:014501-014505.
53. Tucki K, Orynycz O, Wasiak A, Świć A, Mieszkalski L, Mruk R, Gola A, Słoma J, Botwińska K, Gawron J. A Computer Tool Using OpenModelica for Modelling CO2 Emissions in Driving Tests. Energies 2022;15:995.doi.org/10.3390/en15030995
54. Tucki K, Orynycz O, Wasiak A, Świć A, Mruk R. Botwińska K. Estimation of Carbon Dioxide Emissions from a Diesel Engine Powered by Lignocellulose Derived Fuel for Better Management of Fuel Production. Energies 2020;3(3):1-29. doi.org/10.3390/en13030561
55. Tucki K. A Computer Tool for Modelling CO2 Emissions in Driving Tests for Vehicles with Diesel Engines. Energies 2021;14:266. doi.org/10.3390/en14020266
56. Tucki K. A Computer Tool for Modelling CO2 Emissions in Driving Cycles for Spark Ignition Engines Powered by Biofuels. Energies 2021;14:1400. doi.org/10.3390/en14051400